AD/A-002 308

ANGLE-OF-ATTACK EFFECTS ON ELECTRON DENSITY DISTRIBUTION OVER BLUNT BODIES

Henry G. Lew

General Electric Company

Prepared for:

Air Force Cambridge Research Laboratories

July 1974

UNCLASSIFIED

DOCUMENT CONTROL DATA - R & D

(Security classification of title, body of abstract and indexing annotation must be entered when the overall report is classified)

1. ORIGINATING ACTIVITY (Corporate author)
General Electric Company
Re-entry & Environmental Systems Div.
Valley Forge, Pennsylvania 19101

2a. REPORT SECURITY CLASSIFICATION
Unclassified

2b. GROUP

3. REPORT TITLE
ANGLE-OF-ATTACK EFFECTS ON ELECTRON DENSITY DISTRIBUTION OVER BLUNT BODIES

4. DESCRIPTIVE NOTES (Type of report and inclusive dates)
Scientific, Final (Oct. 1971 - Sept. 1974)

5. AUTHOR(S) (First name, middle initial, last name)
Henry G. Lew

6. REPORT DATE	7a. TOTAL NO. OF PAGES	7b. NO. OF REFS
July 1974	29	6

8a. CONTRACT OR GRANT NO.	9a. ORIGINATOR'S REPORT NUMBER(S)
F19628-72-C-0070	GE TIS 74SD2113
8b. PROJECT, TASK, AND WORK UNIT NO. 4642-02-01	
8c. DOD ELEMENT 62101F	9b. OTHER REPORT NO(S) (Any other numbers that may be assigned this report) AFCRL-TR-74-0354
8d. DOD SUBELEMENT 684642	

10. DISTRIBUTION STATEMENT
A - Approved for public release; distribution unlimited.

11. SUPPLEMENTARY NOTES	12. SPONSORING MILITARY ACTIVITY
Tech, Other	Air Force Cambridge Research Laboratories (LZ) Hanscom AFB, Massachusetts 01731 Contract Monitor: John F. Lennon/LZP

13. ABSTRACT

SUMMARY

The electron density distribution over re-entry bodies of the blunt sphere cone class at angle-of-attack to the hypersonic free stream is studied in this report. The shock layer is considered as a mixture of dissociated and ionized air species chemically reacting at finite nonzero rates to produce electrons which are distributed three dimensionally by the nonzero angle-of-attack. Both the viscous three dimensional boundary layer and inviscid flow are included in the study. A numerical implicit finite difference scheme is utilized in the method of solution. Results are given in this report for the hypersonic flow over the AFCRL Trailblazer II body at the angle-of-attack of 12^{o} for the two altitudes of 240,000 ft and 220,000 ft. Additional results for the windward line-of-symmetry are also presented. In general, electron density are predicted to increase with angle-of-attack becoming nonlinear at the higher angles consistent with flight measurements.

DD FORM 1473

UNCLASSIFIED
Security Classification

KEY WORDS	LINK A		LINK B		LINK C	
	ROLE	WT	ROLE	WT	ROLE	WT
Ionized Flow, Viscous Shock Layer, Boundary Layer, Electron Density, Three Dimensional Blunt Body Flow Field, Angle-of-Attack Effects.						

SUMMARY

The electron density distribution over re-entry bodies of the blunt sphere cone class at angle-of-attack to the hypersonic free stream is studied in this report. The shock layer is considered as a mixture of dissociated and ionized air species chemically reacting at finite nonzero rates to produce electrons which are distributed three dimensionally by the nonzero angle-of-attack. Both the viscous three dimensional boundary layer and inviscid flow are included in the study.. A numerical implicit finite difference scheme is utilized in the method of solution. Results are given in this report for the hypersonic flow over the AFCRL Trailblazer II body at the angle-of-attack of 12^{o} for the two altitudes of 240,000 ft and 220,000 ft. Additional results for the windward line-of-symmetry are also presented. In general, an increase in electron density is predicted which becomes nonlinear at the higher angles-of-attack. This prediction is consistent with flight measurements.

PREFACE

The author is grateful for the discussions and comments of John F. Lennon, Contract Monitor, AFCRL.

TABLE OF CONTENT

I. INTRODUCTION

Hypersonic flight of vehicles in the atmosphere produces a layer of electrons which envelopes the entire body. The presence of high electron densities in this layer prevents communication through the vehicle shock layer. The alleviation of this attenuation of electromagnatic signals through the ionized layer can be achieved when an understanding of the electron density distribution exists. The prediction of shock layer ionization at high altitudes for the AFCRL Trailblazer II vehicle was initiated in reference 1 for flow over the body at zero angle-of-attack. High electron concentrations are obtained from the ionization and dissociation of air molecules at temperatures up to $10,000^{\circ}K$. Reference 1 contains the distribution of these electrons about the body taking into account viscous effects at high altitudes. Energy interchange among the molecular air species or with the body surface can change the magnitude of the electron density. The effect of vibrational relaxation of the O_2 and N_2 molecules on the production of electrons was considered in reference 2. At the altitudes of concern for the AFCRL Trailblazer II vehicle flight higher electron density can be caused by the vibrational nonequilibrium states of the molecular species. Other effects such as wall catalyticity and the inclusion of additional molecular and atomic ions besides NO^+ are important factors; these are considered also in reference 2.

The presence of a nonzero angle-of-attack in the flight of the AFCRL Trailblazer II vehicle leads to asymmetry of the flow resulting in an increased pressure on the windward plane and divergence of the surface streamliner from the inviscid streamlines. Both of these phenomena may increase the magnitude of the electron density.

Electron production in the three dimensional laminar nonequilibrium boundary layer on blunt conical bodies such as the AFCRL Trailblazer II vehicle is considered in this report. This is Part II of a two-part report on this problem. Part I, reference 3, contains the basic equations and the method of solution; numerical results at the stagnation line with the effect of a nonzero angle-of-attack were included.

This report contains the numerical results for the electron density distribution over the entire body including additional results at the stagnation line for a nonzero angle-of-attack.

II. EQUATIONS OF MOTION OF A THREE DIMENSIONAL CHEMICALLY REACTING BOUNDARY LAYER OVER A BLUNT BODY

The equations of motion involve the conservation laws for mass, momentum, and energy with diffusion of species reacting at finite chemical rates to produce electrons. A set of orthogonal curvilinear coordinates is utilized fixed to the body such that x is measured along the body generator from the nose of the body and z is the meridional angle in a direction normal to x. The coordinates x and z are surface coordinates; the coordinate normal to the surface is y.

The boundary layer equations for the three dimensional flow with chemical production and diffusion of species are:

$$\rho\left(\frac{du}{dt} - \frac{w^2 r'}{r}\right) = -\frac{\partial p}{\partial x} + \frac{\partial}{\partial y}\left(\mu \frac{\partial u}{\partial y}\right) \tag{1}$$

$$\rho\left(\frac{dw}{dt} + \frac{uwr'}{r}\right) = -\frac{\partial p}{r\partial z} + \frac{\partial}{\partial y}\left(\mu \frac{\partial w}{\partial y}\right) \tag{2}$$

$$\rho \bar{c}_p \frac{dT}{dt} = u\frac{\partial p}{\partial x} + \frac{w}{r}\frac{\partial p}{\partial z} + \mu\left[\left(\frac{\partial u}{\partial y}\right)^2 + \left(\frac{\partial w}{\partial y}\right)^2\right] + \frac{\partial}{\partial y}\left(k\frac{\partial T}{\partial y}\right) + \sum_{i=1}^{N} \rho D_i \frac{\partial c_i}{\partial y}\frac{\partial h}{\partial y} - \sum_{i=1}^{N} w_i h_i \tag{3}$$

$$\rho \frac{dc_i}{dt} = \frac{\partial}{\partial y}\left(\rho D_i \frac{\partial c_i}{\partial y}\right) + w_i, \quad i = 1, 2, \ldots, N. \tag{4}$$

The convective operator is defined by

$$\frac{d}{dt} = u\frac{\partial}{\partial x} + \frac{w}{r}\frac{\partial}{\partial z} + v\frac{\partial}{\partial y} \tag{5}$$

In the above equations the symbols have the following meaning: u, v, and w are the velocity components along the x, y, z coordinates respectively, ρ the mass density, k the heat conductivity, μ the viscosity coefficient, $\bar{c}_p$ the specific heat coefficient at constant pressure of the gas mixture, D_i (i = 1, 2, ... N) the binary diffusion coefficients, r the local radius of the body with the prime indicating differentiation with respect to x, p the pressure, T the temperature, h_i the species enthalpy and, c_i the species concentration in mass fraction. The gas properties are functions of the temperature T and the species concentration. The term w_i is the mass rate of production of the ith species per unit volume for each reaction. The equation of state for the gas mixture is given by:

$$p = R\rho T \sum_{i=1}^{N} c_i/M_i \tag{6}$$

where R is the universal gas constant and M_i is the species molecular weight. The number of species is denoted by N. Finally, the global conservation of mass equation is satisfied. Chemical rates are prescribed for the w_i term and are given in Part I for the dissociated and ionized air species system. These equations together with chemical rate constants, thermodynamics, and transport properties given in Part I are sufficient to determine the (4 + N) unknowns.

The windward line-of-symmetry equations are obtained from eqs. (1) to (4) in the limit of the coordinate z = 0. A series in the z-coordinate for each dependent variable, can be utilized for obtaining this set of equations. The angular velocity component w vanishes to the first power of z and since the edge velocity w_e also vanishes at z = 0 to the first power the ratio (w/w_e) is finite and this variable replaces w in eq. (2).

One notes that the axial momentum retains the same form as that at zero angle-of-attack. The dependent variable in the second momentum equation is essentially the gradient of the angular velocity in the azimuthal direction. The global conservation equation has only an additional term when the angle-of-attack is not zero.

III. METHOD OF PREDICTION

The basic equations of motion for the three dimensional boundary layer utilized in this study have been given; see also Part I. (ref. 3). In that reference the method of solution by finite differences has also been discussed. Moreover, the chemical and thermodynamic data were given there. These considerations were discussed for both the viscous and inviscid edge conditions. As explained in ref. 3 the initial profiles are prescribed from the results at zero angle-of-attack which were obtained previously and given in ref. 1. Thus the three dimensional boundary layer at a nonzero angle-of-attack develops under edge conditions which have partially accounted for the swallowing of the viscous layer at the frontal portion of the body such as that considered in ref. 3. One notes also that the latter result is developed from a fully viscous flow with shock slip at the stagnation point. With initial conditions provided thus, the inviscid edge conditions with finite rate chemistry and the effect of angle-of-attack are obtained first. The boundary layer at the lines of symmetry and along each meridian is then determined. The pressure distribution is presumed known and one set is suggested for use and discussed in Part I. In the discussion which follows the (x, y, z) coordinate system is body oriented with center at the nose of the sphere cone body. To repeat, the x coordinate is measured from the nose, the y coordinate normal to the surface of the body, and z is the azimuthal coordinate. The corresponding transformed coordinates are (ξ, η, ζ) and as given by eq. (2.8) of Part I.

All results given in this report are for the altitudes of 240,000 ft and 220,000 for the AFCRL Trailblazer II vehicle (9° blunted cone with nose radius of .5275 ft) flying at a velocity of 17,500 ft/sec. One notes that this vehicle is a blunt short body with a bluntness ratio of 0.664.

IV. RESULTS AND DISCUSSION

4.1 Windward Line of Symmetry

The angular velocity component (normal to the meridian plane) is zero at the lines of symmetry at both the windward and leeward planes. However, the gradient of this component has a nonzero value, so that the ratio of this velocity to the corresponding inviscid

velocity component is finite. The equations of motion along the line-of-symmetry where both the angular coordinate ζ and the angular velocity w are zero are obtained from equations (1 to 4). As pointed out before the equations at $\zeta = 0$ are of the same form as the zero angle-of-attack ones except for the presence of the second momentum equation and one additional term in the mass conservation equation. These terms are the principal causes in changing the distribution of characteristics along the lines-of-symmetry.

The peak electron density distribution along the body at 240,000 ft altitude and 17,500 ft/sec for several values of angle-of-attack is shown on Figure 1. It is remembered that the flow is symmetrical about wind oriented coordinates over most of the spherical nose. Thus the initial decay of the electron density along x is the same for the angles-of-attack shown. For comparison with the previous results in ref. 1 at zero angle-of-attack the air species considered in Fig. 1 were taken to be 0_2, N_2, N, 0, NO, NO+ and electrons. It is seen that there is more than an order-of-magnitude increase in electron density at the location X = 2.5 ft at 12^o as compared with the 0^o angle-of-attack. Most of this increase is due to an increase of the pressure values in the boundary layer at angle-of-attack.

The corresponding distribution of peak values of atomic species within the boundary layer is shown on Fig. 2. This is typical of the behavior for flow over blunt conical bodies. One notes that the edge values are those of the body streamline aft of the spherical nose consistent with the boundary layer approximation; a partial swallowing of the inviscid streamlines at the frontal portion of the body has been included. For the short body of concern here the production of atomic species is controlled principally by the initial profiles, i.e., temperature and species distribution within the layer, and to a lesser degree by the edge values downstream of the swallowing point. Thus the behavior of this distribution is close to that obtained if the additional swallowing of streamlines at the rear of the body are also included.

The peak electron density for the altitude of 220,000 ft is compared with that of 240,000 ft for the angle-of-attack of 12^o in Fig. 3. There is about an order increase in electron density with this change in altitude as in the zero angle-of-attack case; the

difference in ambient density between the two altitudes is only a factor of about 2.5.

The distribution of electron density normal to the body surface is given on Fig. 4. The coordinate η is the transformed coordinate normal to the surface and is defined in Part I. Results for several values of angles-of-attack are shown on this figure. The electron density has increased by an order-of-magnitude from 2^{o} to 20^{o}. Due to the cold wall condition, the electron density peaks a short distance from the wall at a location about 20% of the total boundary layer thickness.

The variation of peak electron density with angle-of-attack is shown on Fig. 5. for $x = 2.5$ ft at the windward line-of-symmetry. It becomes non-linear with increasing angle-of-attack. The value at zero angle-of-attack was obtained from previous work given in ref. 1 and contains the effect of additional swallowing of the inviscid streamlines toward the rear of the body.

4.2 Inviscid Edge Conditions

The inviscid edge conditions were obtained following the method discussed in Part I. These were obtained for prescribed surface pressure distributions and the integration of the three dimensional inviscid equations by a predictor-corrector method.

The angular velocity distribution is shown on Fig. 6 for several angles-of-attack showing an increase with the angle-of-attack. The angular velocity is zero, of course, at the two lines-of-symmetry. The magnitude of the angular velocity is almost a factor of 1/4 of the axial velocity at 12^{o}. The parameter $w_e/5u_e$ measures the significance of the flow induced by the nonzero angle-of-attack; it has a finite value at both lines-of-symmetry. It decreases with x as the axial velocity increases on the conical portion of the body (of Fig. 7). First order effects due to angle-of-attack vary directly with this parameter. Clearly, this parameter indicates large values of angular velocity compared

with the axial velocity at the higher angles-of-attack with a subsequent appreciable modification of the direction of the flow. The edge conditions of temperature and species concentration were obtained similarly by integration at each point of the body and utilized for input for the boundary layer.

4.3 Distribution of Electrons Over the Body at Angle-of-Attack

Complete boundary layer characteristics were obtained for the AFCRL Trailblazer II body at an angle-of-attack of 12^{o} for the two altitudes of 240,000 ft and 220,000 ft flying at a velocity of 17,500 ft/sec. The method of computation involves first obtaining the inviscid edge conditions over the entire body utilizing the method described previously in Part I. The initial profiles in the spherical region of the body where the flow is symmetrical were obtained from the zero angle-of-attack results. As pointed out before, these profiles contain the effects of swallowing from the stagnation point up to the initial point. The initial profiles for the meridians off the line-of-symmetry were generated from those in the symmetrical portion of the flow. With these initial conditions the windward line-of-symmetry boundary layer characteristics were obtained. Thus initial profiles are now available along two lines normal to each other, that is, the stagnation line-of-symmetry meridian curve and the surface curve normal to this meridian. Finally, the entire flow field was obtained utilizing these initial conditions.

The variation of peak electron density around the body at the angle-of-attack of 12^{o} is shown on Fig. 8 for the altitude of 240,000 ft; Fig. 9 shows the corresponding result at 220,000 ft. The coordinate $\zeta = 0$ is at the windward line-of-symmetry. The electron density decreases in value going from the windward line-of-symmetry to the leeward side for a nonzero angle-of-attack. The decay with distance along each meridian curve of the body follows the same trend as that along the $\zeta = 0$ line. It is interesting to note that the azimuthal variation of the parameter $(w_e/\zeta u_e)$ vary from about 0.35 to 0.37 from $\zeta = 0$ to $\zeta = \pi$. This correspond to a value of the azimuthal velocity component as large as 1/10 of the axial component. Typical azimuthal variation is shown on Fig. 10; and depend strongly on both the pressure and temperature which also decrease with ζ. The azimuthal

pressure and temperature at the edge of the boundary layer are given on Fig. 11. To complete the discussion, Fig. 12 show characteristics such as velocity, temperature and species concentration. The behavior of these characteristics, in general, follow that expected of a three dimensional boundary layer. The pressure in the region along the body at nonzero angle-of-attack windward meridian is higher than that at zero angle-of-attack; correspondingly, the pressure is lower at the leeward line-of-symmetry. The level of pressure is one factor directly proportional to the electron density; thus the electron density is higher at the windward line-of-symmetry. In addition, the air flow is driven by the pressure gradient and this convects fluid with their characteristics from the windward meridian toward the leeward side. This accounts for an additional change in the electron density in the nonzero angle-of-attack case. The angular velocity component is also shown on Fig. 12 and has almost the same form as the axial velocity. For example, the value of $w_e/5u_e$ is 0.1478 at ζ = 1.06 rad. and this leads to the value of w_e/u_e of 0.246. This value of the velocity ratio indicate that the flow is definitely not a small cross flow one. These results are typical and the discussion is aimed at delineating the prinicipal effects of nonzero angle-of-attack in the production of electrons in the shock layer of blunt bodies. Additional numerical results and details are contained in ref. 4.

Flight data measurements at nonzero angle-of-attack have been obtained at AFCRL and some results have been given in ref. 5. The comparison of theoretical predictions given here with these and additional flight measurements will be made by AFCRL; comparison to date indicate a good correlation as noted by Hayes (ref. 6).

V. CONCLUDING REMARKS

A prediction method for determining the effect of angle-of-attack on the electron density distribution over blunt bodies at hypersonic speeds has been developed and studied in this report. This study has included finite rate chemical reactions between dissociated and ionized air species in addition to the effect of three dimensional flow. The numerical results indicate the following:

1. Electron density along the windward line-of-symmetry increases with angle-of-attack and becomes nonlinear with larger angles-of-attack.

2. The velocity component normal to the meridian curve is a large fraction of the axial velocity at 12^{o} and is not a small cross flow.

3. The electron density decreases from the windward line-of-symmetry toward the leeward line-of-symmetry; a decrease by a factor of five at 12^{o} angle-of-attack for both the 240,000 ft. and 220,000 ft. altitudes is obtained.

4. A method has been developed to obtain characteristics of three dimensional boundary layer flow over blunt conical bodies flying at hypersonic speeds at high altitudes which considers finite rate chemistry of dissociated and ionized air species in the production of electrons. Thus more complicated problems which may include the ablation of body material into the boundary layer which can react with the air species to produce additional electrons or new species can be easily studied by this method.

VI. REFERENCES

1. Lew, H. G., Shock Layer Ionization at High Altitude, AFCRL 70-0702 (GE 70SD872), Nov. 1970.

2. Lew, H. G., A Study of Electron Density Distribution in Viscous Flows, AFCRL 72-0718 (GE 72SD2189), Nov. 1972.

3. Lew, H. G., Electron Density Distribution Over Blunt Bodies in Three Dimensional Flow, AFCRL TR-73-0671 (GE 73SD2180), Oct. 1973.

4. Lew, H. G., Hypersonic Viscous Shock Layer Ionization at High Altitude, Data Mem 4 (GE) 1974.

5. Hayes, D. T. and Rotman, W., Microwave and Electrostatic Probe Measurements on a Blunt Re-entry Vehicle, AIAA Journal, Vol. II, No. 5, 675-682 (1973).

6. Hayes, D. T., personal communication, 1974.

VII. LIST OF FIGURES

Figure

1. Peak Electron Density Distribution Along the Body at the Altitude of 240,000 ft and Velocity of 17,500 ft/sec for the Angles-of-Attack of 2^{o}, 6^{o}, and 12^{o} at the Windward Line-of-Symmetry.

2. Peak Values of the Atomic Species Along the Body at 240,000 ft., 17,500 ft/sec for Angles-of-Attack of 2^{o}, 6^{o}, and 12^{o} at the Windward Line-of-Symmetry.

3. Peak Electron Density Distribution Along the Body for Two Altitudes of 240,000 ft. and 220,000 ft. at an Angle-of-Attack of 12^{o}.

4. Electron Density Distribution at the Windward Symmetry Line for the Altitude of 240,000 ft. and Velocity of 17,500 ft./sec.

5. Variation of Electron Density With Angle-of-Attack at the Windward Symmetry Line

6. Distribution of Angular Velocity Around the Body for Several Angles-of-Attack at 240,000 ft., 17,500 ft./sec. at X = 2.5 ft.

7. The Angular Velocity Parameter $w_\theta/5u_\infty$ For Flow at 240,000 ft, 17,500 ft./sec. at X = 2.5. ft.

8. Decay of the Electron Density at Each Meridian Around the Body at an Altitude of 240,000 ft. and Velocity of 17,500 ft./sec. for a 12° Angle-of-Attack.

9. Decay of Electron Density at Each Meridian Around the Body at an Altitude of 220,000 ft. and Velocity of 17,500 ft./sec. for 12° Angle-of-Attack.

10. The Distribution of Electron Density Around the Body at an Altitude of 240,000 ft. and a Velocity of 17,500 ft./sec. for 12° Angle-of-Attack.

11. Azimuthal Variation of Temperature and Pressure at the Boundary Layer Edge at the Altitude of 240,000 ft. and Velocity of 17,500 ft./sec. for 12° Angle-of-Attack.

12. Azimuthal Variation of Characteristics of the Boundary Layer at the Altitude of 240,000 ft. and Velocity of 17,500 ft./sec.

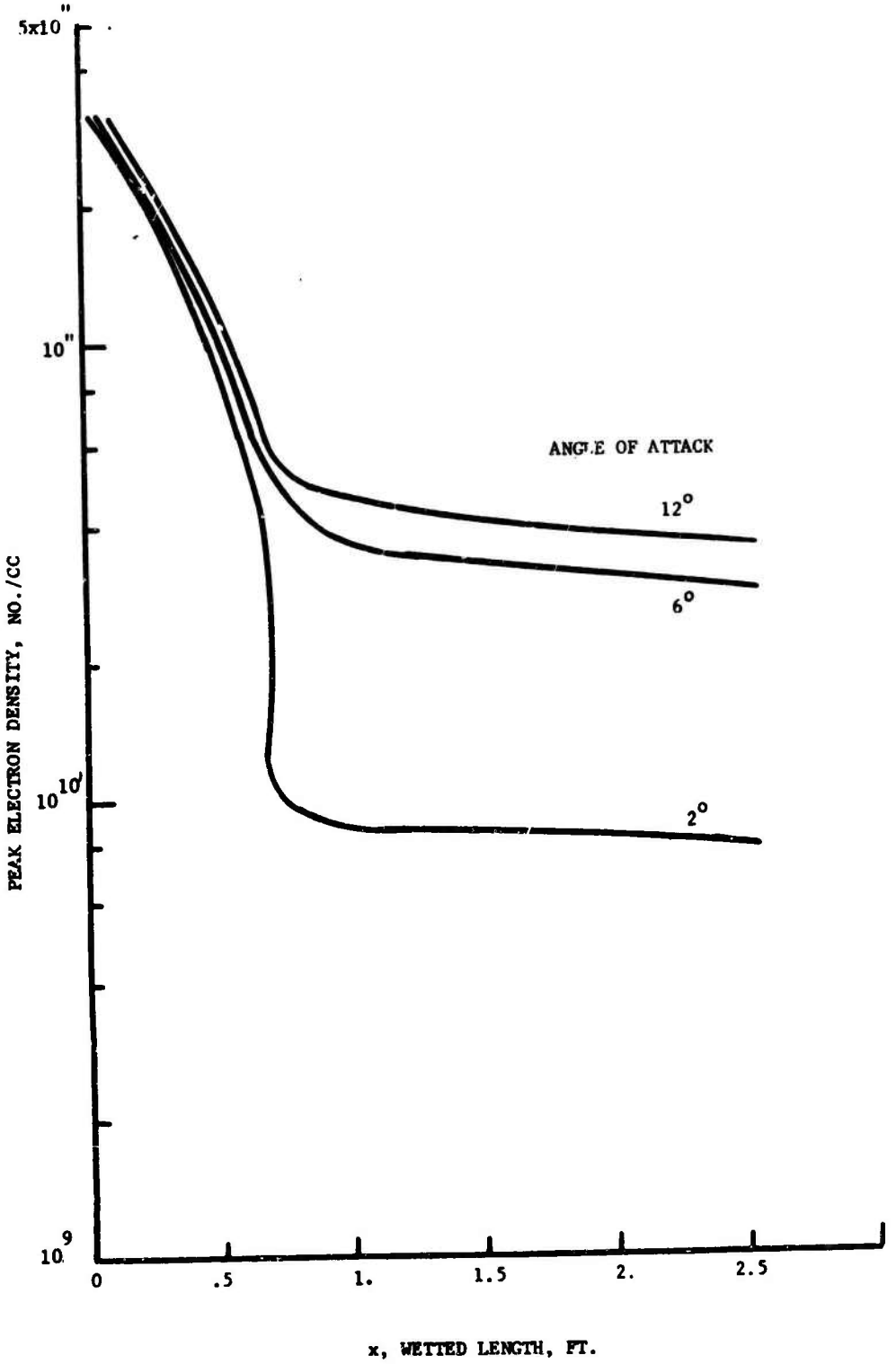

FIGURE 1: PEAK ELECTRON DENSITY DISTRIBUTION ALONG THE BODY AT THE ALTITUDE OF 240,000 FT. AND VELOCITY OF 17,500 FT/SEC FOR THE ANGLES-OF-ATTACK OF 2°, 6°, AND 12° AT THE WINDWARD LINE-OF-SYMMETRY.

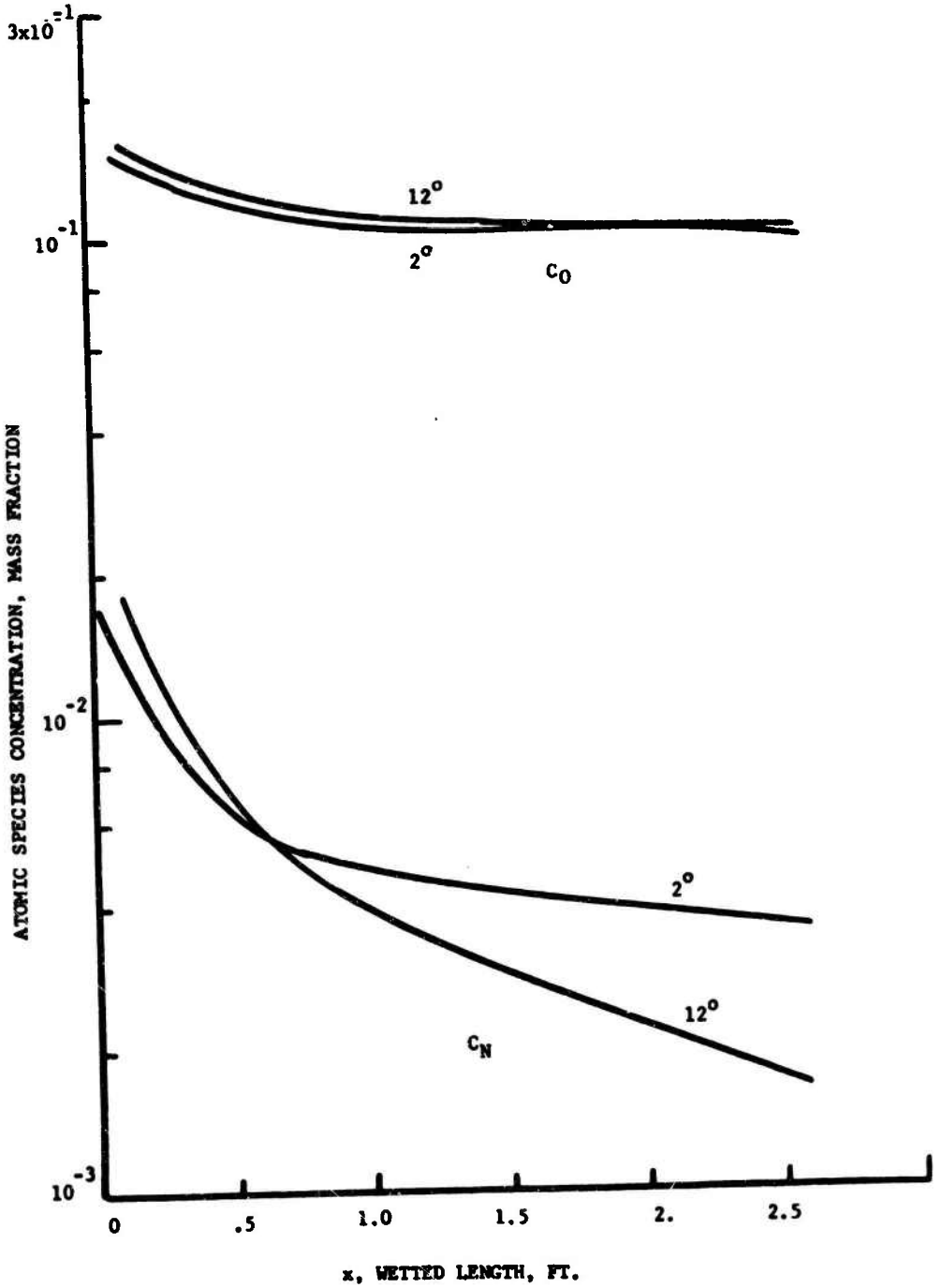

FIGURE 2: PEAK VALUES OF THE ATOMIC SPECIES ALONG THE BODY AT 240,000 FT_δ, 17,500 FT/SEC FOR ANGLES-OF-ATTACK OF 2°, 6°, AND 12° AT THE WINDWARD LINE-OF-SYMMETRY.

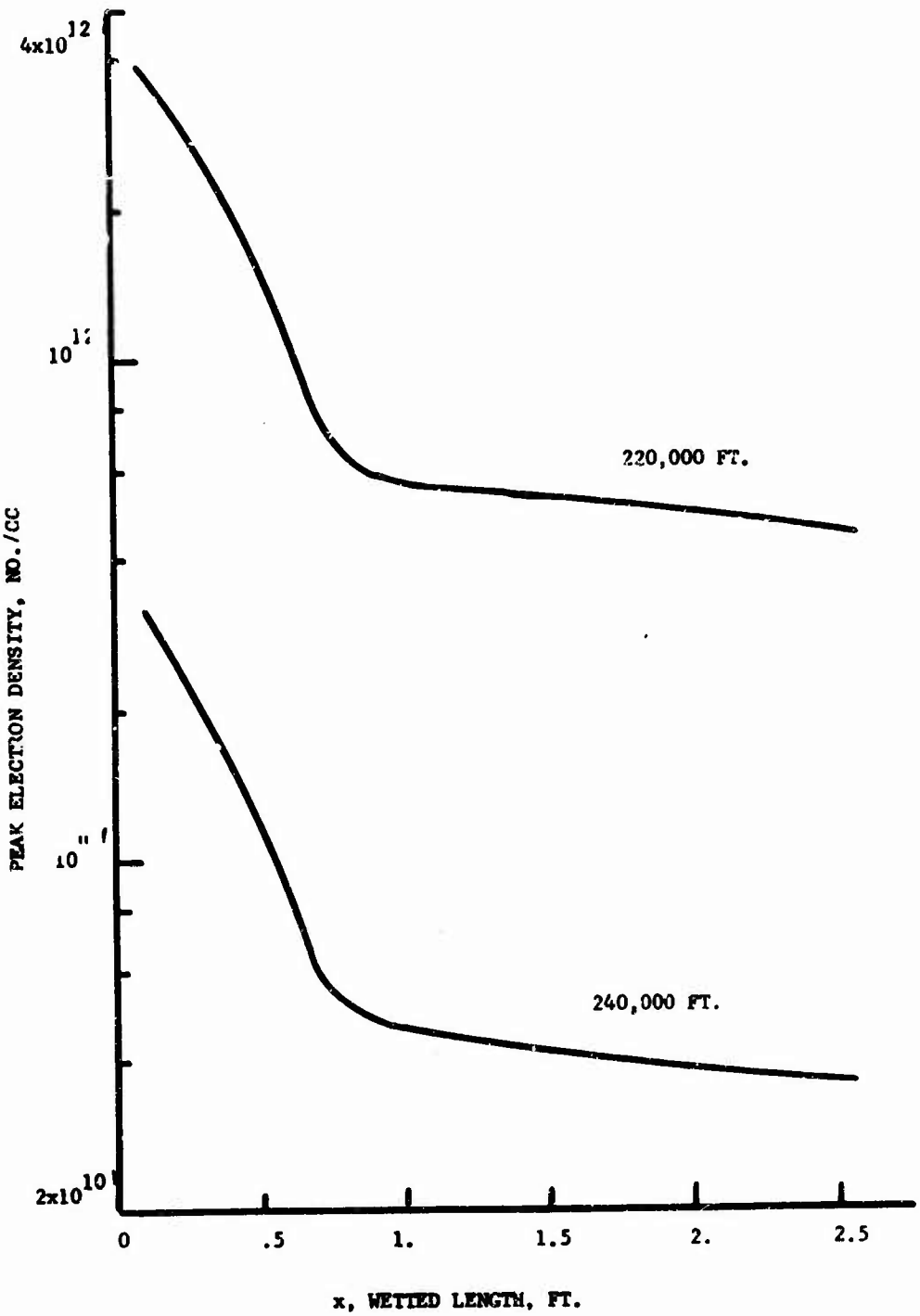

FIGURE 3: PEAK ELECTRON DENSITY DISTRIBUTION ALONG THE BODY FOR TWO ALTITUDES OF 240,000 FT. AND 220,000 FT. AT AN ANGLE-OF-ATTACK OF 12°.

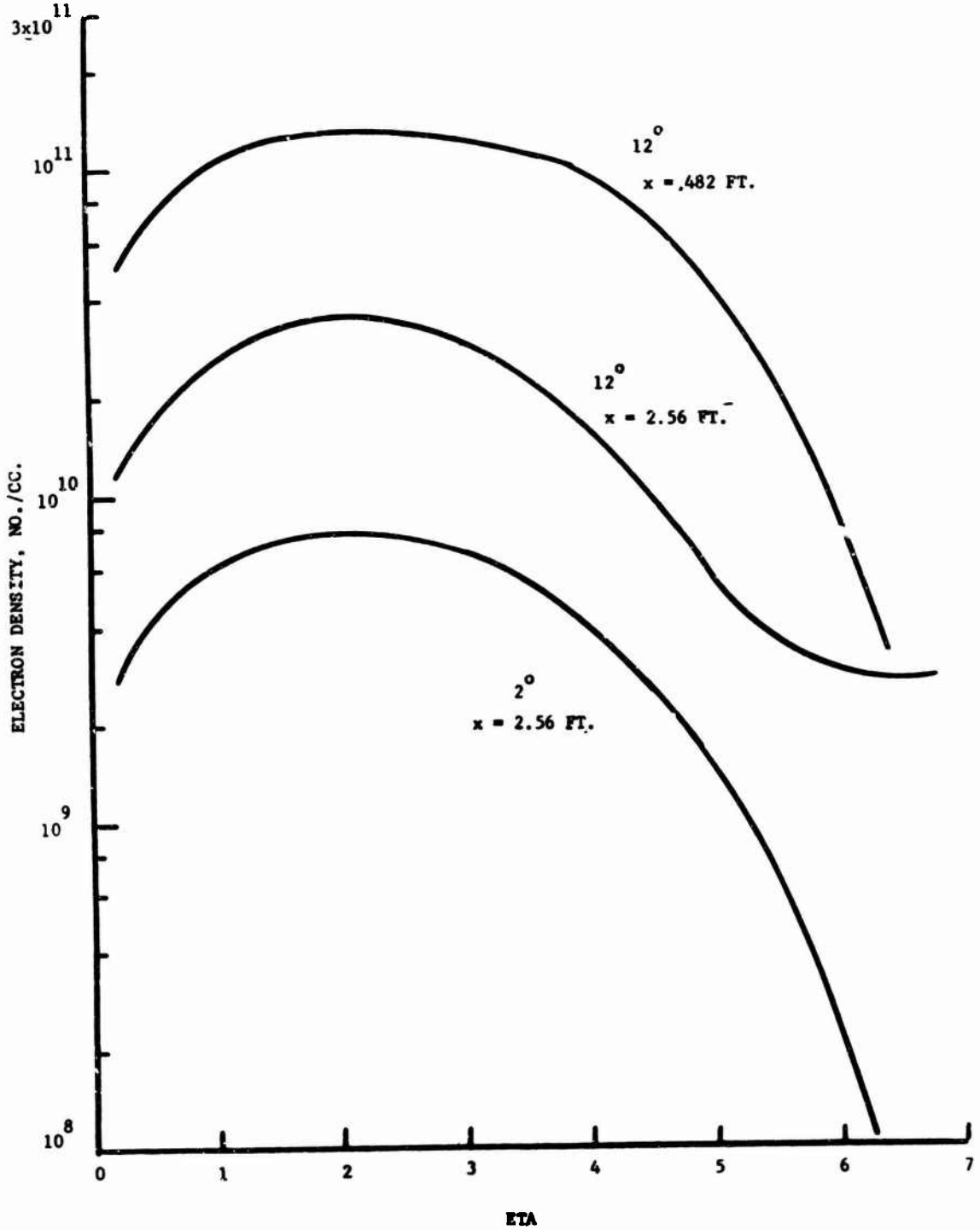

FIGURE 4: ELECTRON DENSITY DISTRIBUTION AT THE WINDWARD SYMMETRY LINE FOR THE ALTITUDE OF 240,000 FT. AND VELOCITY OF 17,500 FT/SEC.

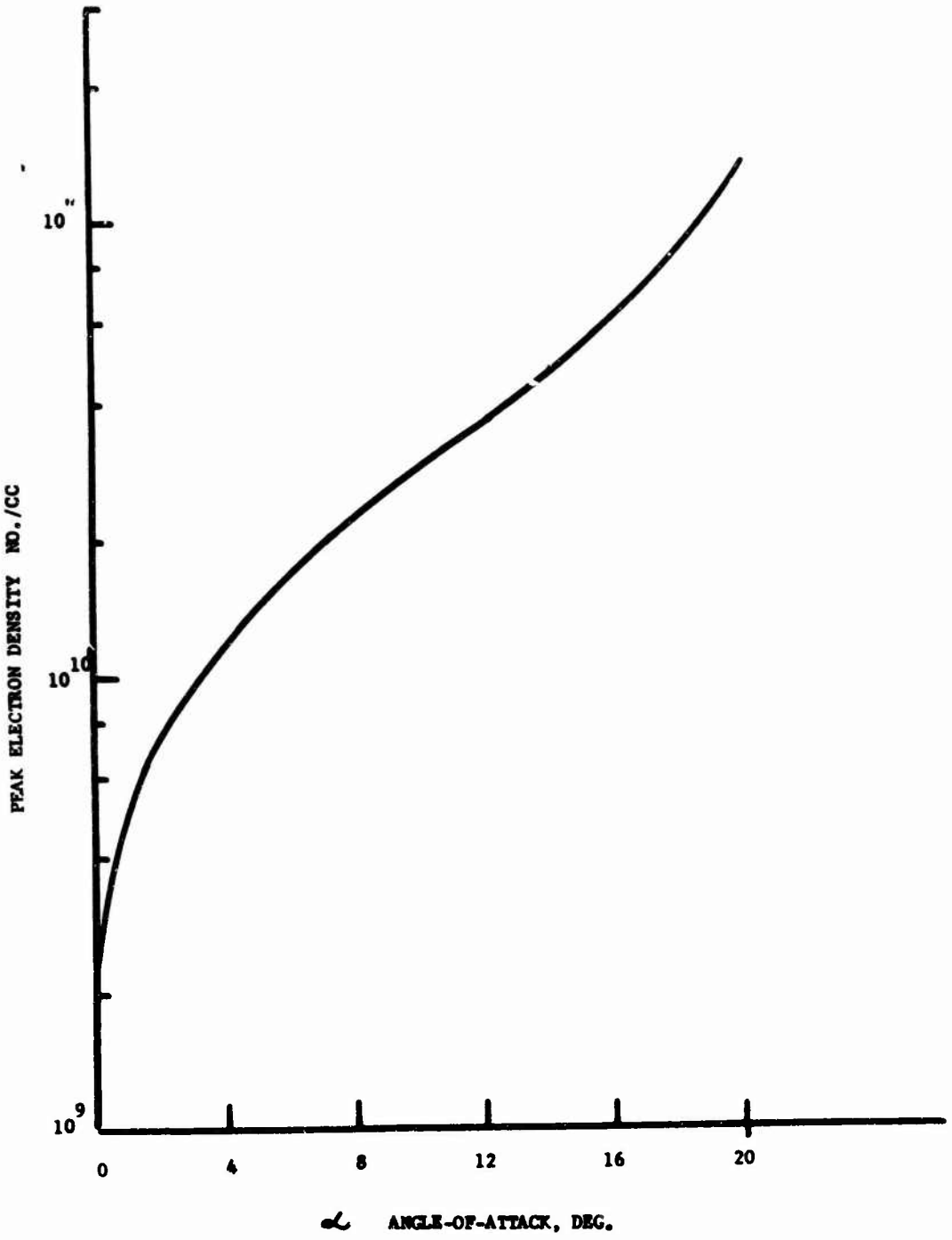

FIGURE 5: VARIATION OF ELECTRON DENSITY WITH ANGLE-OF-ATTACK AT THE WINDWARD SYMMETRY LINE.

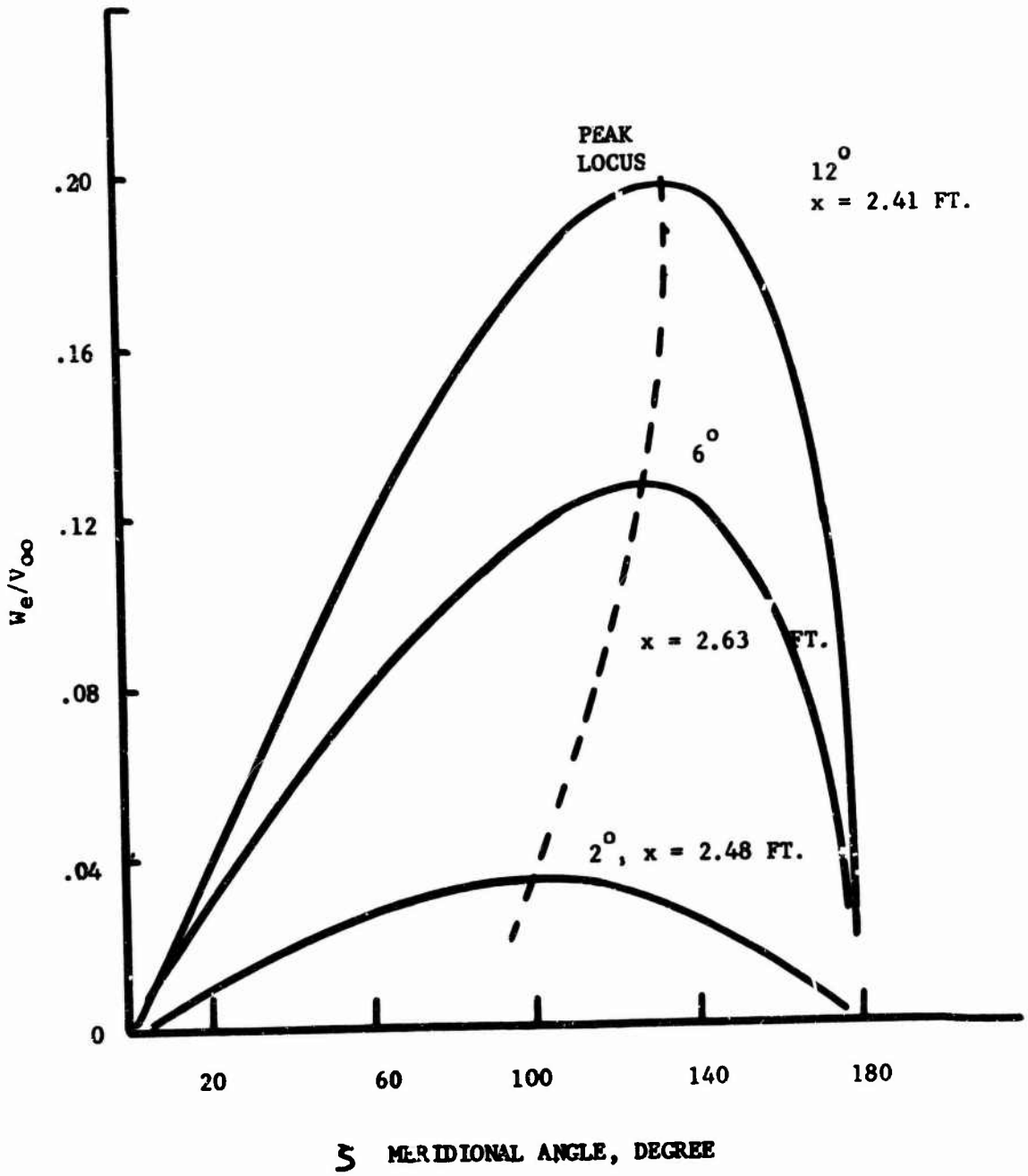

FIGURE 6: DISTRIBUTION OF ANGULAR VELOCITY AROUND THE BODY FOR SEVERAL ANGLES-OF-ATTACK AT 240,000 FT., 17,500 FT/SEC AT X = 2.5 FT.

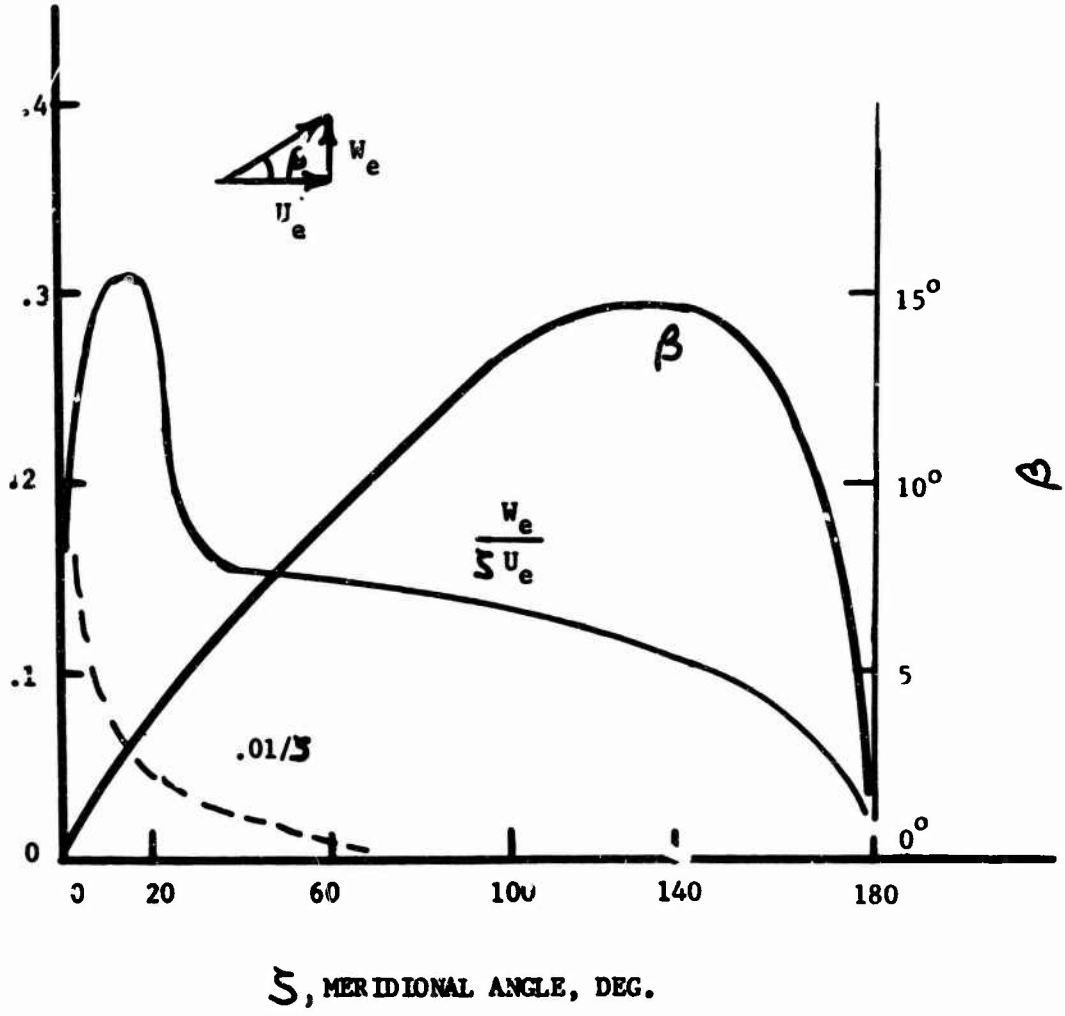

FIGURE 7: THE ANGULAR VELOCITY PARAMETER $W_e/\zeta U_e$ FOR FLOW AT 240,000 FT., 17,500 FT/SEC AT X = 2.5 FT.

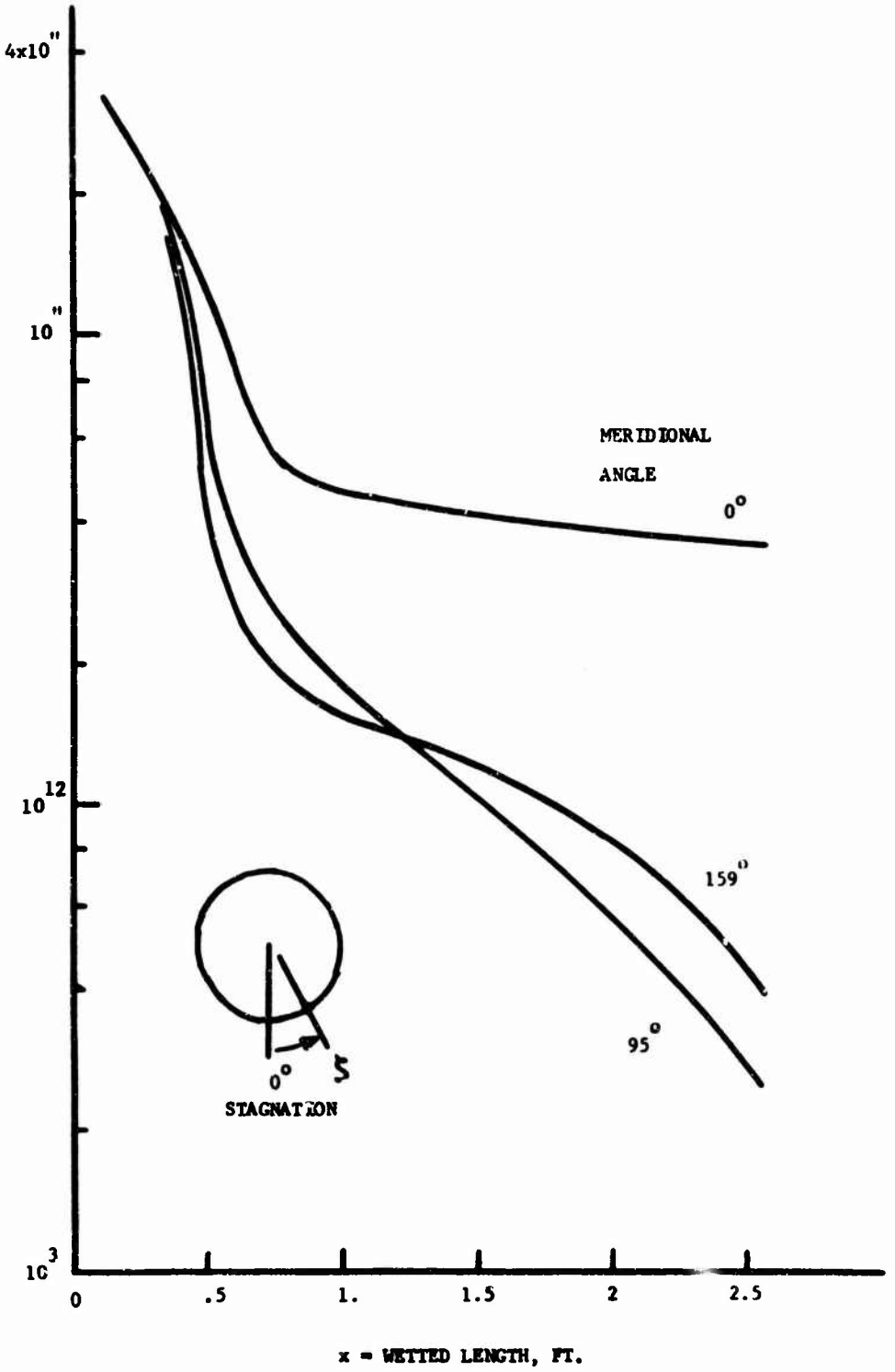

FIGURE 8: DECAY OF THE ELECTRON DENSITY AT EACH MERIDIAN AROUND THE BODY AT AN ALTITUDE OF 240,000 FT. AND VELOCITY OF 17,500 FT/SEC FOR A 12° ANGLE-OF-ATTACK.

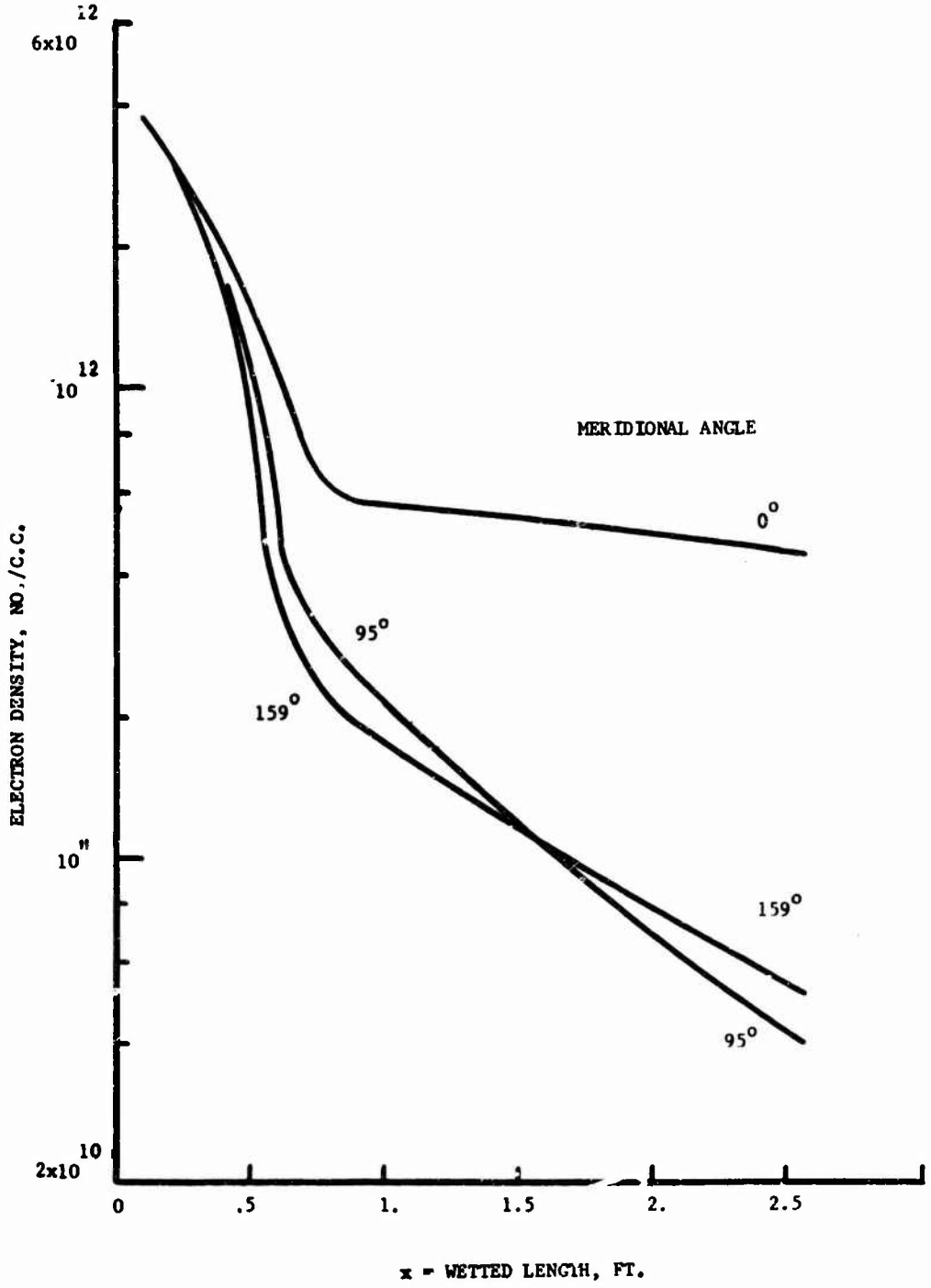

FIGURE 9: DECAY OF ELECTRON DENSITY AT EACH MERIDIAN AROUND THE BODY AT AN ALTITUDE OF 220,000 FT. AND VELOCITY OF 17,500 FT/SEC FOR 12° ANGLE-OF-ATTACK.

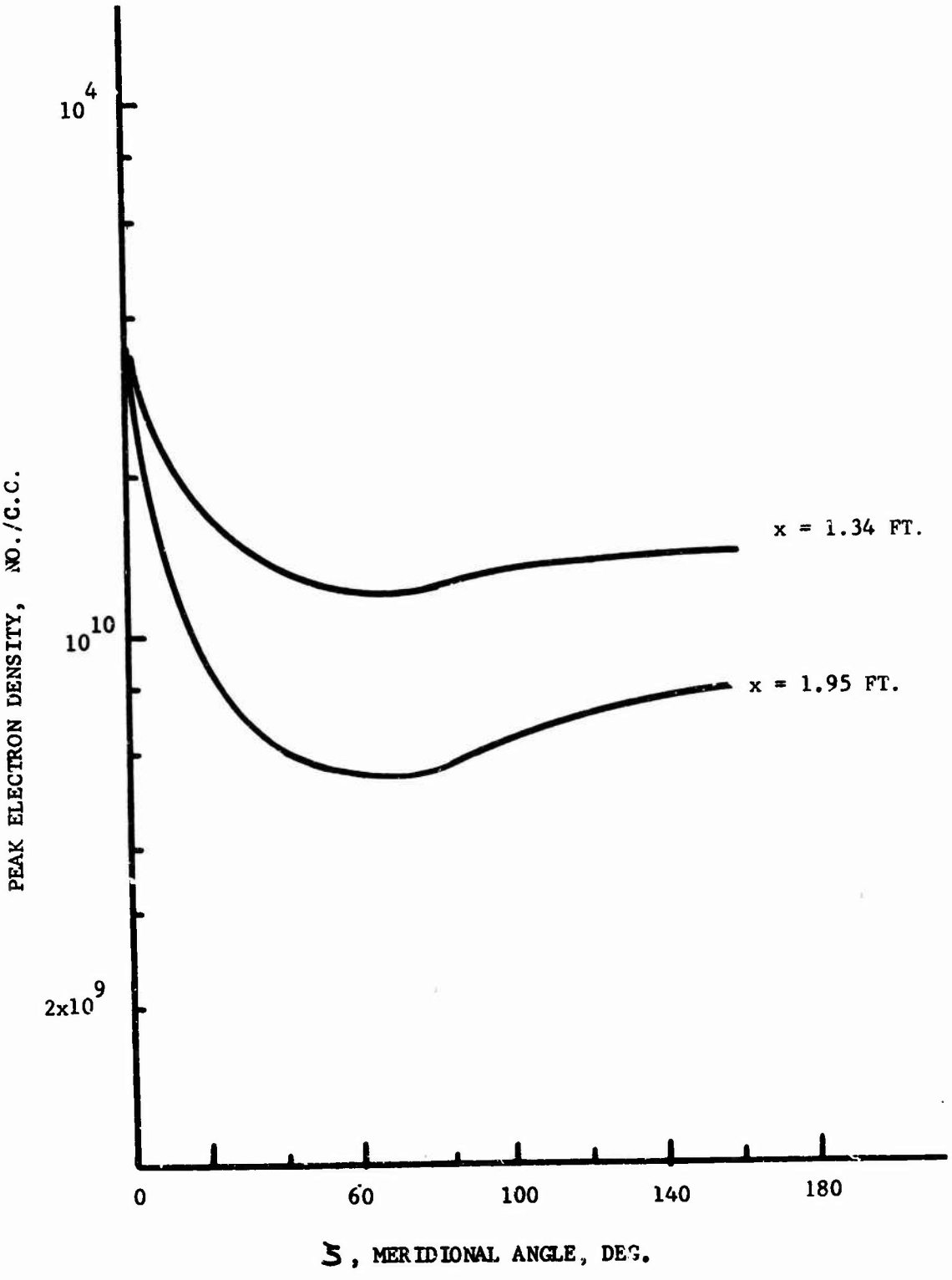

FIGURE 10: THE DISTRIBUTION OF ELECTRON DENSITY AROUND THE BODY AT AN ALTITUDE OF 240,000 FT. AND A VELOCITY OF 17,500 FT/SEC FOR 12° ANGLE-OF-ATTACK.

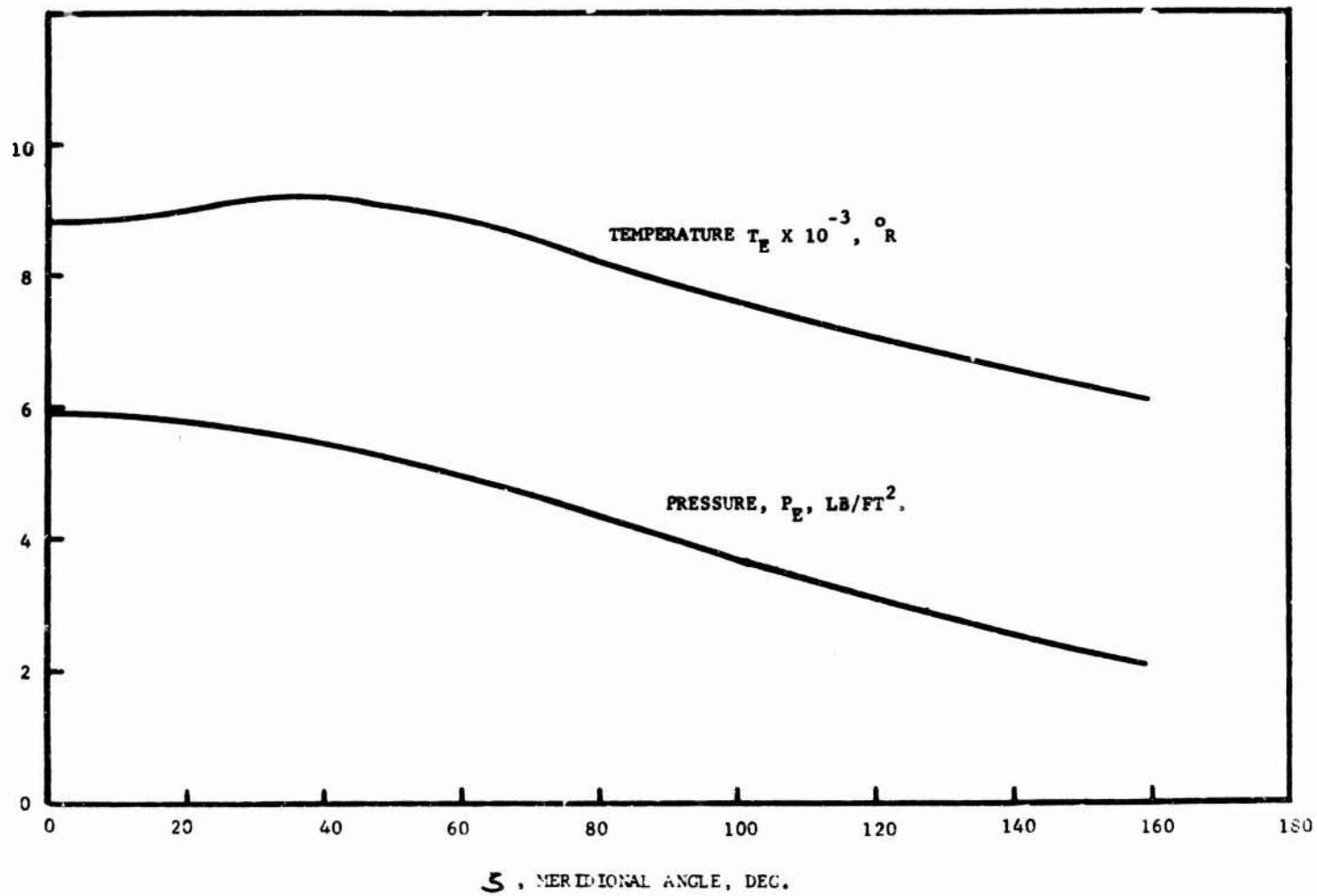

FIGURE 11: AZIMUTHAL VARIATION OF TEMPERATURE AND PRESSURE AT THE BOUNDARY LAYER EDGE AT THE ALTITUDE OF 240,000 FT. AND VELOCITY OF 17, 500 FT/SEC FOR 12° ANGLE-OF-ATTACK.

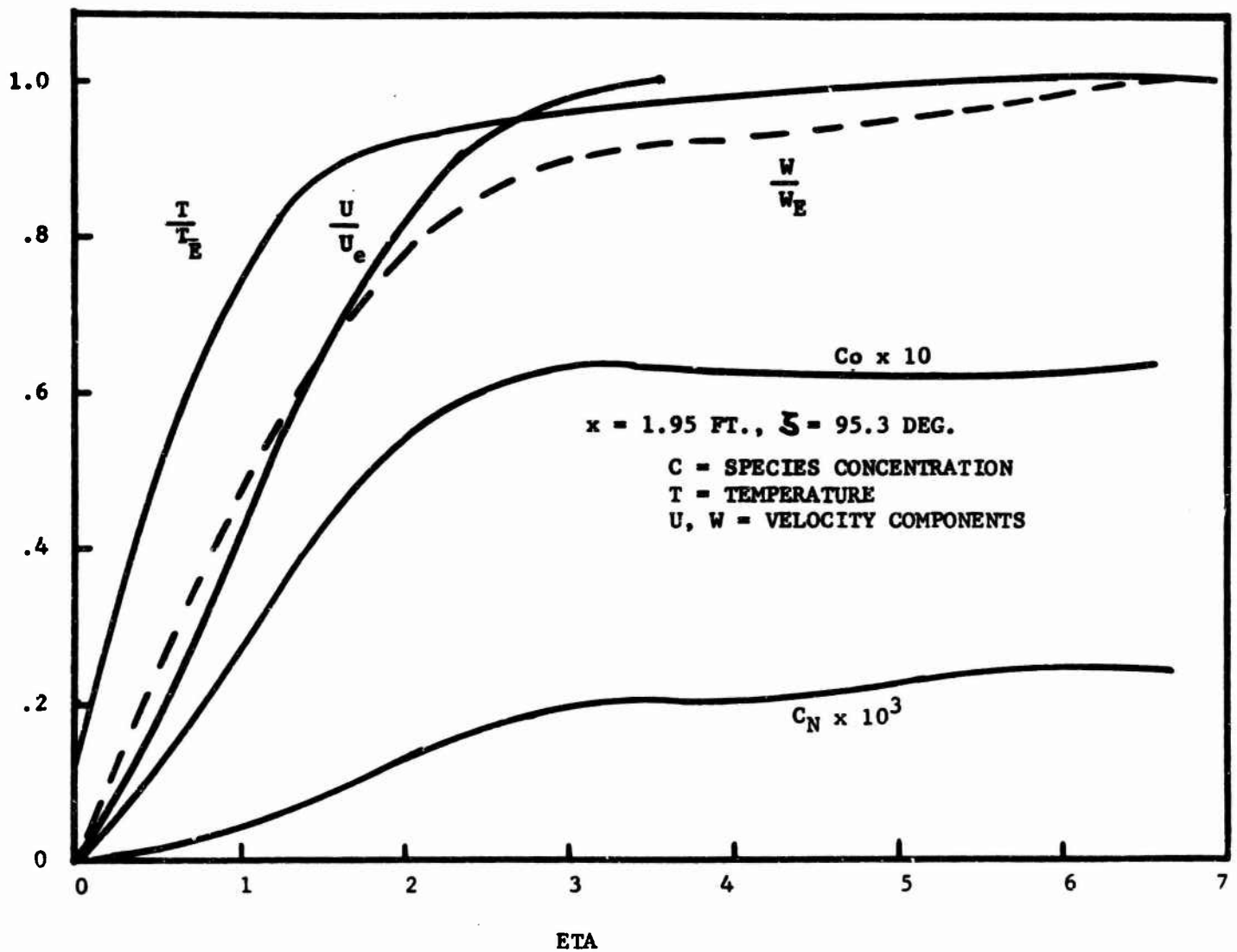

FIGURE 12: AZIMUTHAL VARIATION OF CHARACTERISTICS OF THE BOUNDARY LAYER AT THE ALTITUDE OF 240,000 FT. AND VELOCITY OF 17,500 FT/SEC.